Universiteit
Leiden
The Netherlands

Shape analysis for phenotype characterisation from high-throughput imaging

Guo, Y.; Guo Y.

Citation
Guo, Y. (2017, October 17). *Shape analysis for phenotype characterisation from high-throughput imaging*. *SIKS Dissertation Series*. Retrieved from https://hdl.handle.net/1887/56254

Version:	Not Applicable (or Unknown)
License:	Licence agreement concerning inclusion of doctoral thesis in the Institutional Repository of the University of Leiden
Downloaded from:	https://hdl.handle.net/1887/56254

Note: To cite this publication please use the final published version (if applicable).

Cover Page

Universiteit Leiden

The handle http://hdl.handle.net/1887/56254 holds various files of this Leiden University dissertation

Author: Guo Yuanhao
Title: Shape analysis for phenotype characterisation from high-throughput imaging
Date: 2017-10-17

Chapter 5

Multi-modal 3D Reconstruction

Based on:

- Y. Guo, R.C. van Wijk, E.H.J. Krekels, H.P. Spaink, P.H. van der Graaf & F.J. Verbeek, "Multi-modal 3D reconstruction and measurements of zebrafish larvae and its organs using axial-view microscopy," in IEEE Conference on Image Processing, Beijing, China, 2017.

This chapter addresses RQ 5.

> **RQ 5**: *How can we obtain a multi-modal 3D description and the corresponding measurements for the zebrafish from the MM-HTAI architecture?*

Abstract – In life sciences, light microscopy is used to study specimens. On the organism-level a bright-field representation presents an overview for the whole shape of a specimen; the organ-level fluorescent staining representation insightfully supports in the interpretation of the detailed intrinsic structures (see Section 5.1). We apply our MM-HTAI architecture presented in Chapter 3 (see Subsection 3.3.1) to acquire axial-view images for the organism and organs of zebrafish larvae (See Subsection 5.2.1). We obtain multi-modal 3D reconstruction using the shape-based method, from which we can derive the 3D measurements of volume and surface area (see Subsection 5.2.2). In this method, we employ a microscope camera calibration using voxel residual volume maximization algorithm. We intuitively align and fuse the obtained multi-models (see Subsection 5.2.3). Experimental results show natural visualisation both for the whole organism and organ of zebrafish larvae; subsequently accurate 3D measurements are obtained (see Section 5.3). The method is very suitable for high-throughput research in which knowledge on size and shape is relevant to the understanding for development, effects of compounds or drugs (see Section 5.4).

5.1 Multi-modal 3D reconstruction

In modern life-sciences research, e.g., developmental biology, (patho)physiology, toxicology, and pharmacology, light microscopy is commonly used to produce 2D colour representations of biological phenomena. Zebrafish is a popular vertebrate model organism in biomedical research because of its many advantages, among which is optical transparency at early stages [11, 123]. The organs of the transparent larvae can be studied *in vivo* through microscopy. Transgenic lines are available that express a fluorescent reporter gene in specific organs, tissues, or cell types [16]. In this way, organ development of the genetically engineered zebrafish can be visualised and monitored over time by fluorescence microscopy. It makes the zebrafish particularly suitable for large scale screening experiments using light microscopy. For the screening of large libraries of compounds for organ toxicity, such as hepatotoxicity [23], quantitative endpoints like organ size or growth retardation are required. In order to accurately evaluate the shape and size of an organ like the liver, 3D modelling of both the liver and the whole organism are required. Compared with 2D imaging, 3D measurements, e.g., size, volume and surface area, are more reliable. The organism-level imaging is an overview of the shape of the object, serving as shape reference to normalise the 3D measurements of liver into unit metrics. Our aim is to develop a method for 3D reconstruction and measurements of zebrafish larvae and its organs using axial-view microscopy.

In stereo vision, a 3D scene can be recovered by matching correlated multi-view images [30]. This is implemented by pixel-level searching [102] or salient point detection and matching [124]. However, these methods are challenged for our typical application at hand, the zebrafish. Here, partial transparency of the zebrafish complicates straightforward application of these methods as it is difficult to match the implicit surface points on the object. Based on the concept of visual hull [125], the space carving algorithm reconstructs the 3D shape from a range of 2D binary shapes [126], which is also referred to as the silhouette-based 3D reconstruction [80, 81]. In a sample population of zebrafish, a rather large colour variation exists; this holds both for bright-field and fluorescence. Therefore, we propose to use 2D binary representations. Accordingly, we have developed the profile-based 3D zebrafish reconstruction method based on a series of 2D axial-view shapes of the object, obtaining a precise 3D representation and accurate 3D measurements in various larval stages [98].

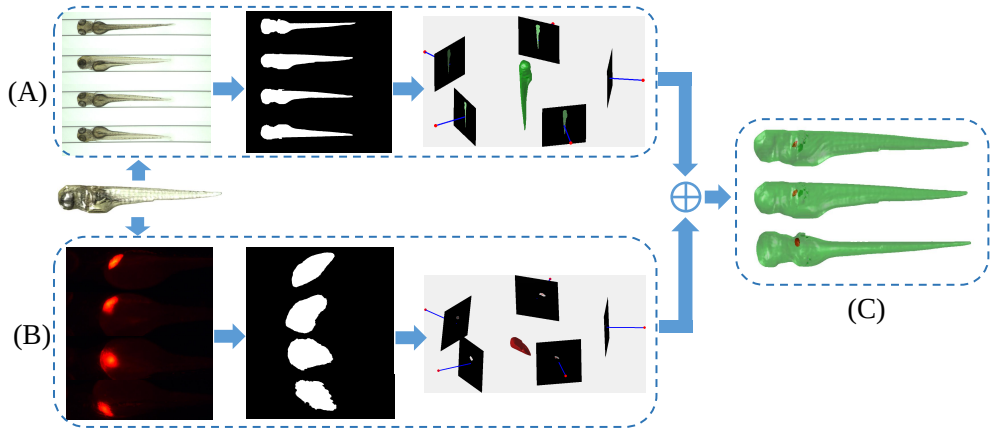

Figure 5.1: A schema of the proposed method. One zebrafish larva presents in the two imaging pipelines. (A) The organism-level 3D reconstruction. (B) The organ-level 3D reconstruction. (C) The multi-modal 3D reconstruction fusion and visualisation. In (A) and (B), the first columns show the original axial-view images; the second columns illustrate the 2D binary shapes; the third columns denote the camera system calibration and profile-based 3D reconstruction.

In Chapter 3 (see Subsection 3.3.1), we have implemented our MM-HTAI architecture. In this chapter, using the axial-view images acquired from this multi-modal imaging modality, we propose a multi-modal 3D reconstruction method as presented in Fig. 5.1. A zebrafish larva with fluorescent marker expressed in the liver is captured in two imaging modes. The VAST camera enables the organism-level imaging and a microscope camera facilitates the organ-level imaging. From the axial-view images, 2D binary shapes are obtained through modern segmentation algorithms [28, 29]. We estimate the camera projection geometry for the two camera systems using the voxel residual volume maximization algorithm. We produce the multi-modal 3D reconstruction for the organism (zebrafish) and organ (liver) using the profile-based 3D reconstruction method; we use heuristics to fuse the two models acquired from different imaging modalities. From the obtained 3D models, 3D measurements, e.g., volume and surface area, are derived.

5.2 Our approach

In this section, we present a new dataset containing the zebrafish on both organism- and organ-level imaging (see Subsection 5.2.1). We introduce the microscope camera calibration and elaborate shape-based 3D reconstruction (see Subsection

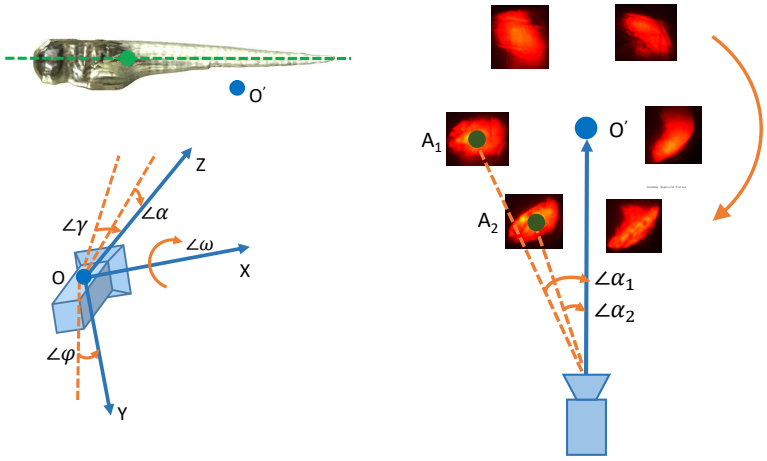

(a) (b)

Figure 5.2: (a) The VAST camera pose is modelled as the 3D transformation from the camera centre O to the object centre (green circle). The green line denotes the profile-axis along which the object revolves. $\angle\omega$, $\angle\varphi$ and $\angle\gamma$ represents the 3D rotation angles of the camera along the X, Y and Z directions, respectively. $\angle\alpha$ is modelled as the "translation angle". (b) The centre of the zebrafish liver is not aligned with the zebrafish centre which results in its rotation and revolution with respect to the zebrafish centre, such that the "translate angle" $\angle\alpha$ of the microscope camera is specified for each view.

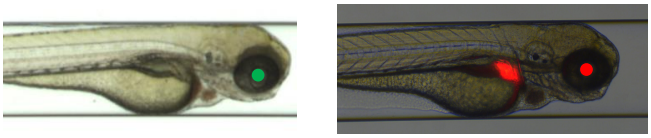

Figure 5.3: The alignment of the multi-modal 3D reconstruction is implemented according to the iris centre of the zebrafish. On the left-side is a bright-field image of organism-level imaging. We crop this image to fit the space. On the right-side is a bright-field image overlaid with a fluorescent image of organ-level imaging.

5.2.2). We present an interactive method to align and fuse the multi-modal 3D reconstruction (see Subsection 5.2.3).

5.2.1 Dataset collection

In Chapter 4, we have collected three datasets using our MM-HTAI architecture. We extend *Dataset C* in this chapter. We use the VAST camera in our MM-

HTAI architecture to obtain bright-field images presenting the whole shape of the zebrafish larvae. For the same specimens, we use the imaging modality of fluorescent microscopy in our MM-HTAI architecture to obtain images presenting the zebrafish liver. We used the imaging protocol in accordance with Chapter 4. In this manner, we obtain multi-modal images for the same group of specimens. This further facilitates our multi-modal 3D reconstruction.

5.2.2 Shape-based 3D reconstruction

In this subsection, we apply our shape-based 3D reconstruction approach to obtain the multi-modal 3D reconstruction for our specimen, i.e., the zebrafish larvae and its livers. More details for the methodology can be found in Subsection 3.3.3 and 3.3.4. We have learned that a good shape-based 3D reconstruction is conditioned to a feasible microscope camera calibration. In Subsection 3.3.5, this has been done by the voxel residual volume maximisation (VRV) algorithm. However, in this chapter, a proper adaption for the method should be made. As shown in Fig. 5.2 (a), the revolution centre of the specimen is aligned with its centre of the profile-axis. This benefits the camera system parameterisation, because "translation angle" can be shared by all the virtual cameras. In Fig. 5.2 (b), one can see that the motion of the zebrafish liver is a mixture of the rotation along the centre of the zebrafish profile-axis and the revolution along its own centre. Accordingly, we just need to specify the "translation angle" for each view in the microscope camera calibration. The optimisation for the VRV algorithm again can be solved by the Nelder-Mead simplex method [90]. In this manner, we separately perform the camera calibration in the two imaging modalities, i.e., the VAST-camera and the microscope camera.

5.2.3 3D multi-models alignment and fusion

The 3D models are obtained from different imaging modes. So, we need to align the resulting multi-modal 3D reconstruction as part of the fusion operation. During the organ-level imaging, we acquired bright-field images in register with the fluorescent images. These images only partially depict the object, but provide a good reference for alignment. We have obtained the camera poses for both models from camera calibration. So, we choose the same axial-view for the zebrafish and localise the iris centre as shown in Fig. 5.3. We use the organ-level 3D model

as a template. The organism-level 3D model is scaled, rotated, and shifted to align with the former according to the camera pose and the position of the iris centre.

For a view of the zebrafish liver, we use its corresponding bright-field microscopic image to localise the iris centre for the specimen represented as $\mathbf{l}_1$; we choose the same axial-view for VAST image for the same zebrafish and localize the iris centre represented as $\mathbf{l}_2$. In this subsection, we use index 1 and 2 to separately represent the organ-level and organism-level coordinate frame. These are shown in Fig. 5.3.

According to the camera projection model $\mathbf{P}$, we can find the pixel location $\mathbf{c}$ for the world centre $\mathbf{C}$ defined in the two cases as follows.

$$\begin{cases} \mathbf{c}_1 = \mathbf{P}_1 \times \mathbf{C}_1 \\ \mathbf{c}_2 = \mathbf{P}_2 \times \mathbf{C}_2 \end{cases} \tag{5.1}$$

We can compute the relative displacement for our reference point, i.e., the zebrafish iris centre, with respect to the world centre in the image plane as $\mathbf{d}_1 = \mathbf{l}_1 - \mathbf{c}_1$ and $\mathbf{d}_2 = \mathbf{l}_2 - \mathbf{c}_2$.

Through camera calibration, we have known the accurate focal length f of the camera and the translation F along the principal line from world centre to the camera centre. Using 3D geometry, we can find the coordinates of the two reference points in 3D world frame as:

$$\begin{cases} \mathbf{L}_1 = \mathbf{d}_1 \times \frac{F_1}{f_1} \\ \mathbf{L}_2 = \mathbf{d}_2 \times \frac{F_2}{f_2} \end{cases} \tag{5.2}$$

We use $\mathbf{V}_1$ and $\mathbf{V}_2$ represent the vertices in the triangulated mesh for the 3D modellings of the organ and the organism, respectively. From the calibrated images, we can extract accurate 3D rotation $\mathbf{R}$ for the object with respect to the world centre in our chosen reference view. If we choose the world frame as the template, we need to rotate and translate the world frame for the organism to align the former frame. This is formulated as follows.

$$\mathbf{V}_{2\to1} = \mathbf{V}_2 \times \mathbf{R}^{-1} + (\mathbf{L}_1 - \mathbf{L}_2) \tag{5.3}$$

Where $\mathbf{R}^{-1}$ denotes the inverse rotation for the organism.

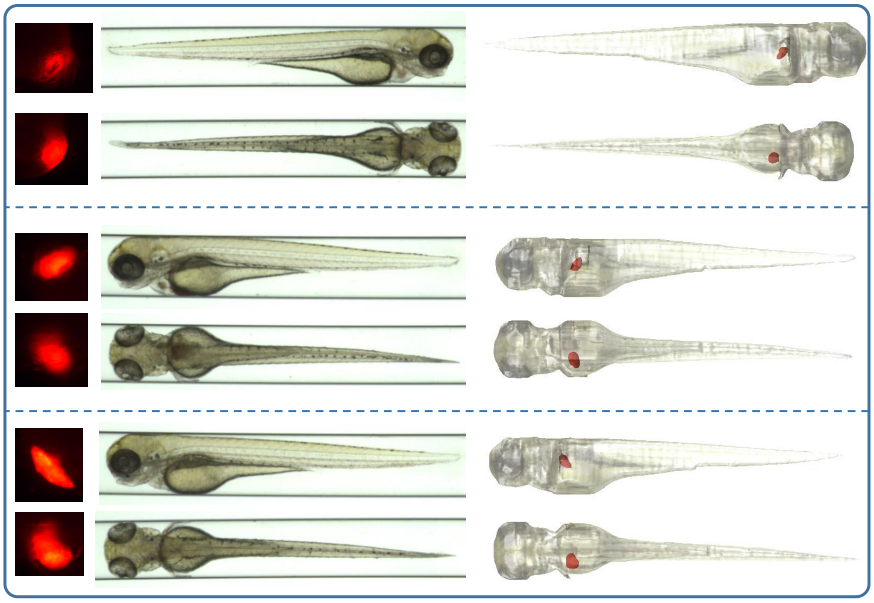

Figure 5.4: Multi-modal 3D reconstruction visualisation. We selected three examples from our dataset and for each example we visualise two typical views (lateral and dorsal). The first column represents fluorescent liver images. The middle column is the zebrafish image in bright-field. The last column visualises the fusion of the multi-modal 3D reconstruction. One can zoom in for a better observation.

Through the above process, we have obtained the aligned 3D model for the organism with respect to the organ. We then visualise the 3D multi-models $\mathbf{V}_1$ and $\mathbf{V}_{2\to1}$ in the same world frame to accomplish the multi-modal 3D reconstruction fusion.

5.3 Experiments

In this section, we apply our method on the zebrafish dataset for performance evaluation. We first visualise some examples of the multi-modal 3D reconstruction in Subsection 5.3.1, and subsequently report on the 3D measurements of volume and surface area for the zebrafish larvae and its liver in Subsection 5.3.2.

Table 5.1: 3D measurements of the 3D reconstructed models for the zebrafish (ZF) and its liver (Liver)

	Volume		Surface area	
	ZF	Liver	ZF	Liver
	($\times 10^8 \mu m^3$)	($\times 10^5 \mu m^3$)	($\times 10^6 \mu m^2$)	($\times 10^4 \mu m^2$)
#1	2.74	7.70	3.33	4.67
#2	2.59	5.38	3.24	3.61
#3	2.50	8.01	3.13	4.91
#4	2.91	9.06	3.44	5.20
#5	2.67	11.60	3.31	6.07
#6	2.80	15.15	3.47	6.89
#7	2.80	6.55	3.41	4.28

5.3.1 Results visualisation

From our dataset, we select three examples for visualisation as shown in Fig. 5.4. Two typical axial-views are shown, i.e., lateral and dorsal, and each example is separated by blue lines. The first column shows the original organ-level fluorescent images. Those images depict the natural shape of the zebrafish liver. One can observe a variation in image quality from the different examples. This is caused by strength of the fluorescent marker. The middle column shows the organism-level bright-field images. The zebrafish are partially transparent but retains explicit contours for the shape. The last column visualises the fusion of the 3D models. For a natural appearance, we map the texture from the zebrafish to the 3D model. We clearly observe the shape of both the zebrafish and its liver. The visual and spatial discernibility of the models are emphasised from the multi-modal fusion. It is interesting that, although the liver is not completely visible in a all views (the first view of the first example), our method still recovers a good 3D shape by imposing a threshold to the confidence score to estimate a 3D model allowing a range of errors. An animated visualisation of the results can be found at `http://bio-imaging.liacs.nl/galleries/VAST-3Dorgan/`.

5.3.2 3D measurements for 3D multi-models

From the multi-modal 3D reconstruction, we derive 3D measurements, i.e., volume and surface area. The volume is obtained by the integration over all the voxels included in the object. A set of surface points is generated from the voxels

by the marching cubes algorithm [121], from which a triangulated mesh can be produced. The obtained 3D surface is further refined [93]. Subsequently, the surface area is obtained by the integration of all the facets in the triangulated mesh using Heron's formula [92]. In Table 5.1 we report on the computed 3D measurements of volume and surface area for both zebrafish and its liver.

In previous work [98], we have reported accurate 3D measurements for the 3 dpf zebrafish, from which we obtained the volume statistics as 2.53 ± 0.11 ($\times 10^8 \mu m^3$) and the surface area as 3.20 ± 0.15 ($\times 10^6 \mu m^2$). In this experiment, the statistics of the 3D measurements for the zebrafish are 2.72 ± 0.14 ($\times 10^8 \mu m^3$) for the volume and 3.33 ± 0.12 ($\times 10^6 \mu m^2$) for the surface area. The phenomenon that the specimens in this experiment are larger compared to our reference set is due to the fact that we did not accurately time the development for this experiment. We also computed the statistics of the 3D measurements for the liver as 9.06 ± 3.33 ($\times 10^5 \mu m^3$) for the volume and 5.09 ± 1.10 ($\times 10^4 \mu m^2$) for the surface area. The shape variation of the zebrafish liver is large for different individuals, but we can observe that a larger zebrafish tends to have a larger liver [127].

We implemented our method using Matlab programming on a desktop with an Intel i7 CPU and a 16G RAM. Subsequently, we evaluated the efficiency as runtime for the 3D reconstruction of the zebrafish and its liver separately as $22.0 \pm 0.4(s)$ $26.3 \pm 1.3(s)$. The results of this experiment can be directly used for establishing physiological values of a healthy liver of a 3 dpf zebrafish. The method can be more generically used to assess all observable effects of any compound on the shape and size of an organ.

5.4 Chapter conclusions and future work

In this chapter, we have presented a method for multi-modal 3D reconstruction and fusion on both organism- and organ-level through light microscopy axial-view imaging. It answers RQ 5: *How can we obtain a multi-modal 3D description and the corresponding measurements for the zebrafish from the MM-HTAI architecture*? We applied our MM-HTAI architecture to extend *Dataset C* presented in Chapter 4 (see Subsection 4.3). We then applied our multi-modal 3D reconstruction method on the dataset. Within the reconstructed 3D models, we observe an overview shape for the object on the organism-level and the detailed structure on the organ-level. The former provides a good shape reference to normalise

and evaluate the organ development in phenotypical research. The experimental results show a natural visualisation of the multi-modal fusion images. Additionally, accurate 3D measurements are obtained, which can be directly used for the evaluation of the biological system with compound screening.

We believe our method is adequate to address RQ 5. However, in near future, we think it can be further developed for the determination of size and shape of other fluorescently labelled organs and objects, such as pathogens or tumour cells. In order to improve this work, a larger sample size of our subjects should be considered to get better statistics for the 3D measurements. High-throughput imaging would also be a good approach for this task.